International Journal of Research
Available at https://edupediapublications.org/journals
e-ISSN: 2348-6848
p-ISSN: 2348-795X
Volume 04 Issue-17
December 2017

Multilevel Inverter based PV/Wind Microgrid

Mrs. M. Nagalakshmi & Mr. P. Ankineeduprasad
M-tech student Scholar Department of Electrical & Electronics Engineering, Vikas group of institutions , Nunna; Krishna(Dt); A.P, India.
Email: mnagalakshmi30@gmail.com
M-tech miste Associate Professor Department of Electrical & Electronics Engineering, Vikas Group of institutions, Nunna, Krishna (Dt); A.P, India.
Email: ankineedupadamata@gmail.com

Abstract:*Photovoltaic (PV) energy has great potential to supply energy with minimum impact on the environment, since it is clean and pollution free. Continuously increasing demand of Microgrid with high penetration of distributed energy generators, specially focused on renewable energy sources is modifying the traditional structure of the electric distribution grid. Renewable energy sources such as PV, wind and fuel cells are usually connected through voltage-source inverters. This paper focuses on the solar energy, grid connected photovoltaic system, modeling of photovoltaic array, maximum power point tracking, and grid connected inverter. The output voltage and current and interfaced to grid system using 2-level, 3-level and 5-level inverter topology. These inverters are connected in parallel and the control strategy has to stabilize the system and achieve good power sharing. The MLI performance can be analyzed by using MATLAB/SIMULINK model.*

Keywords-parallel inverter, stability, microgrid, SVPWM, photovoltaic, wind, Multi Level Inverters (MLI).

I. INTRODUCTION

In recent years, multilevel inverters have gained popularity with medium and high power ratings. Renewable energy sources such as photovoltaic, wind, and fuel cells can be interfaced to a multilevel converter system [1]. Many multilevel converter topologies have been proposed during the last two decades. Research has engaged novel converter topologies and unique modulation schemes.

The three types of multilevel converter structures reported in the literature are: cascaded H-bridge converter with separate dc sources, diode clamped (neutral clamped), andflying capacitors (capacitor clamped). Modulation techniques and control paradigms have been developed for multilevel converters such as sinusoidal pulse width modulation (SPWM), selective harmonic elimination (SHE-PWM), space vector modulation (SVM), and others. The other one is a DC/AC power converter to interconnect the photovoltaic system to the grid. The classical single or three-phase two level voltage source inverter is normally used for this power converter type [2-3]. However, other topologies have been proposed. Multilevel converter topologies are a very interesting choice for realizing this objective.

Multilevel power Converters present several advantages over a conventional two level converter such as: reducing switching frequency, output voltage with very low distortion and reduced dv/dt stress [4-5]. In this way, several multilevel topologies have been applied to photovoltaic systems. This paper gives information about 2 converters structures, analyzing them regarding quality nature of output voltage, harmonic profile, THD values as per IEC standards. It starts with simpler converters and ends with more comprehensive ones, but all of them have the main features: high efficiency, relative low number of semiconductors and the capability to inject energy into the grid without using transformers. Several works have focused on developing PV model and the charge controller. Some of the research efforts also designed power conditioning devices and their controller. This work focuses on the development of a micro- grid model that consists of PV arrays, power conditioning devices and an inverter with overall and individual controller. The model configuration can be tested off-grid or on-grid [6-8].

This paper proposes the grid 5-level inverters are used with PV generation scheme and interfaced to grid system with good voltage profile. Many, multilevel converter applications include industrial medium-voltage motor drives, renewable energy systems with utility interface, flexible AC transmission system (FACTS), and traction drive systems. In grid-connected systems, the panels needed to reach the required power levels are usually arranged in strings. The multilevel inverter requires a separate DC source or single DC source for each bridge; thus, the high power and/or high voltage from the combination of the multiple modules would favor this topology in grid-connected PV applications [9-10]. The multilevel inverter also presents the advantages of reducing the device voltage stress, reducing output filters, and being high efficiency [11-12].

The problem of eliminating harmonics in switching inverters has been the focus of research for many years. The current trend of modulation control for multilevel inverters is to output high quality power with

International Journal of Research
Available at https://edupediapublications.org/journals
e-ISSN: 2348-6848
p-ISSN: 2348-795X
Volume 04 Issue-17
December 2017

high efficiency. For this reason, popular traditional PWM modulation methods are not the best solution for multilevel inverter control due to their high switching frequency. The selective harmonic elimination method has emerged as a promising modulation control method for multilevel inverters. The major difficulty or the selective harmonic elimination method is to solve the equations characterizing harmonics; however, the solutions are not available for the whole modulation index range, and it does not eliminate any number of specified harmonics to satisfy the application requirements. The proposed harmonic elimination method is used to eliminate any number of harmonics and can be applied to DCMLI application requirements [13].

II. MATHEMATICAL MODEL OF PV/WIND MICROGRID

The typical circuit of two parallel three-phase voltage source inverters fed through 10 kWp PV array and 20 kW wind turbine is shown in Figure.1. The controller has to stabilize the system and to have a good power sharing even when the sources have different DC values. This is the situation when the inverters are connected with different renewable sources. According to the learning curve the cost reduction of PV system will continue in the future. PV/Wind MG is proven to be one of the forms of future evolution of the grid. A PV/Wind Microgrid is shown inFigure. 1. The PV source is a series and parallel connections of PV modules. PV modules can be connected to the grid in different configurations such as the central, string and multistring.

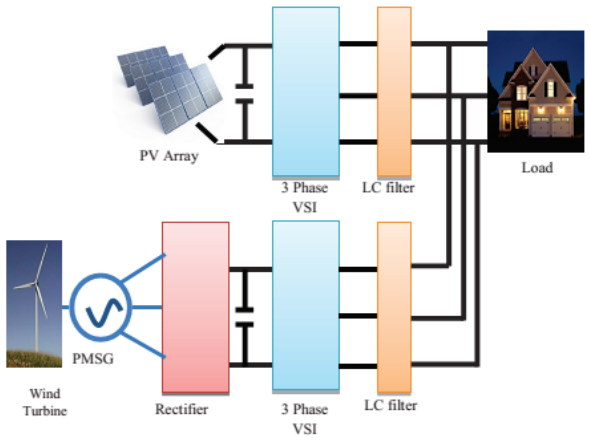

Fig.1. A system of two parallel inverters

a) The Mathematical Model of the PV Array

PV solar cells rely on the photoelectric effect to generate electricity. In the dark the characteristics of the PV cell is similar to the normal diode. When sunlight with energy greater than the semiconductor energy gap hits the cell electrons becomes free and a considerable current flows in theexternal circuit. As PV cells are fragile and have low voltage they grouped into modules and encapsulated from front and supported by metallic panel for protection. The modules are then connected in series and parallel to form an array as shown in Figure 2. There are many methods in the literature for modeling PV modules and 11]. The model used in this paper is based on the single-diode model and extracting some of the parameters from the manufacturer data sheet. The electrical circuit model is shown in Figure 3.

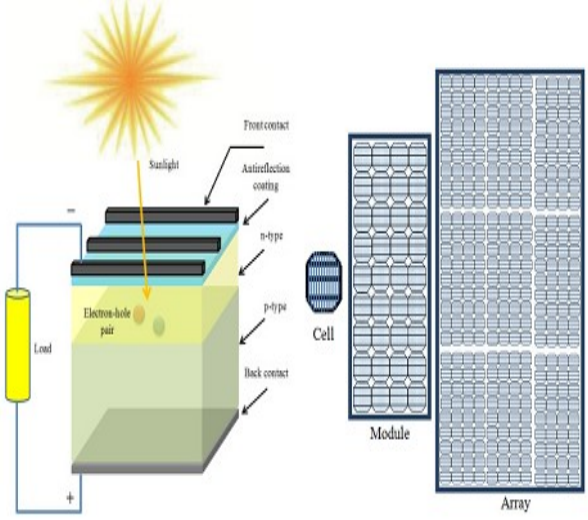

Fig.2. A pn-junction silicon solar cell

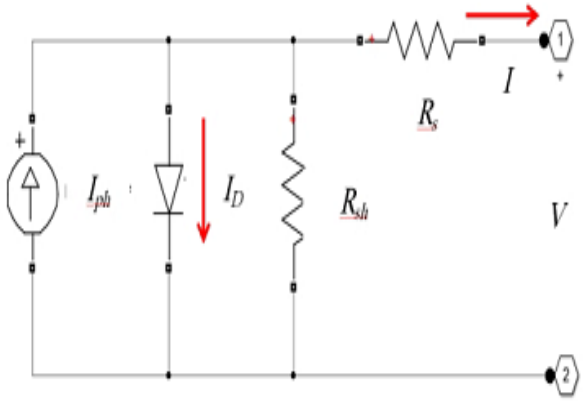

Fig.3. Circuit model of a solar cell

The model is with middle complexity where the temperature dependence of I_0, Iph, and Voc are included. Also the parasitic resistances Rs and Rsh and their temperature dependence are taken into account. The ideality factor is used as a variable to match the simulated data with the manufacturing data. The mathematical model of a solar cell based on the single diode model is given as:

International Journal of Research
Available at https://edupediapublications.org/journals
e-ISSN: 2348-6848
p-ISSN: 2348-795X
Volume 04 Issue-17
December 2017

$$I(T,G,V) = I_{ph} - I_0\left(e^{(V+IR_s)/nV_{th}} - 1\right) - (V + I \cdot R_s)/R_{sh}$$
$$= I_{ph} - I_D - I_{sh} \quad (1)$$

Where the variables in (1) are given by;

$$I_{ph} = I_{ph0} \cdot G / G_{nom} \quad (2)$$

$$I_{ph}(T) = I_{ph} + K_0(T - T_{meas}) \quad (3)$$

$$K_0 = \left(I_{ph}(T_2) - I_{ph}(T_1)\right)/(T_2 - T_1) \quad (4)$$

$$I_0 = I_{SC(T_1)} \cdot (T/T_1)^{3/n} \cdot \exp(-E_g / V_s(1/T - 1/T_1)) \quad (5)$$

$$I_0(T_1) = I_{SC(T_1)} / (\exp(qV_{OC(T_1)} / nkT_1) - 1) \quad (6)$$

$$R_s(T) = -dV/dI_{V_{oc}} - 1/(I_{0(T_1)} \cdot q/nkT_1 \cdot e^{qV_{oc(1)}/nkT_1}) \quad (7)$$

$$R_{sh} = V_{OC}/(I_{ph} - I_0[\exp(qV_{OC}/nkT_{meas} - 1]) \quad (8)$$

$$R_{sh}(T) = R_{sh} \cdot \left(T/T_{meas}\right)^{\alpha} \quad (9)$$

The parameters in the model are explained briefly. Iph is the photo generated current in Amperes. Iph0 is the photogene rated current at the nominal radiation. I_0 is the diode dark saturation current. ID is the diode dark current. Ish is the shunt current. Rs is the series resistance. Rsh is the shunt resistance.G is the solar radiation in W/m^2. The Gnom is the radiation the PV module is calibrated at. n is the ideality factor. e is the electron charge. k is Boltzmann's constant.

Vg is the semiconductor energy gap. K0 is the short-circuit current temperature coefficient. Vth is the thermal voltage. The manufacturer provides the following: Ns: the number of cells in series, Np: the number of cells in parallel, Isc: the short-circuit current, Voc: the open-circuit voltage. The SolarexMSX60 60W module is used in the simulation. The equations from (1) to (9) are implemented in Matlab/Simulink.The PV modules are connected in series and parallel to produce the required voltage and power. As our energy source is nonlinear the goal of the controller is to generate AC power with given voltage shape parameters and to achieve power sharing between the different inverters in the MG. The PVarray used in the simulation has 10 branches with 22 modules in each branch and the total number of modules is 220.

b). The Mathematical Model of the Wind Turbine

The mechanical power of the wind turbine is given by:

$$P_m = 0.5\rho A C_p v_w^3 \quad (10)$$

Where Pm the mechanical power in watts, is the air density (Kg/m^3), A is the swept area (m^2) and Cp is the power coefficient of the turbine, v_w is the wind speed (m/s). The power coefficient represents the conversion efficiency of the turbine. If the pitch angle β=0, Cp is function of the tip speed, λ, of the turbine and is given by:

$$C_p(\lambda) = c_1\left(\frac{c_2}{\lambda} - c_4\right)e^{-c5/\lambda} + c_6\lambda \quad (11)$$

where$\lambda=\omega R/v_w$, ω is the rotational speed (rad/s), R is theradius of the blades. The maximum power can be extractedfrom the turbine can be achieved when cp=0.48 and λ=8.1. The coefficients c1 to c6 are: c1 = 0.5176, c2 = 116, c3 = 0.4, c4 = 5,c5 = 21 and c6 = 0.0068 [13]. The wind turbine used in the simulation has the following specification: power rating, 20kW, the rated wind speed 12 m/s, cut-in and cut-out speeds 5and 25 m/s respectively, blade diameter 10 m. The mechanical power of the wind turbine versus the generator speed for different wind speeds is shown in Figure 4.

c) The Permanent Magnetic Synchronous Generator

The mathematical model of the PMSG is given by:

$$di_d/dt = v_d/L_{ds} - (r_s/L_{ds})i_d + (L_{qs}/L_{ds})\omega_e i_q \quad (12)$$

$$di_q/dt = v_q/L_{qs} - (r_s/L_{qs})i_q + (L_{ds}/L_{qs})\omega_e i_d - (\psi_f \omega_e/L_{qs}) \quad (13)$$

$$T_e = 1.5\,p(L_{ds} - L_{qs})i_d i_q + i_q\psi_f \quad (14)$$

where, Ld, Lq are d and q axis inductances, R is stator winding resistance, id, iq are d and q axis currents, vq, vd are d and q axis voltage, ωr is angular velocity of rotor, λm is amplitude ofrotor induced flux, p is pole pair number, and Te iselectromagnetic torque. The specification of the PMSG are as follows: Ld = Lq = 0.95 mH, the stator resistance Rs=0.085**Ω**,the inertia 0.08 Kg.m^2, the viscous damping 0.001147 N. m. snubber of poles 4. The output electrical AC power of thePMSG is converted into DC power through the diode rectifieras shown in Figure.5.

International Journal of Research
Available at https://edupediapublications.org/journals
e-ISSN: 2348-6848
p-ISSN: 2348-795X
Volume 04 Issue-17
December 2017

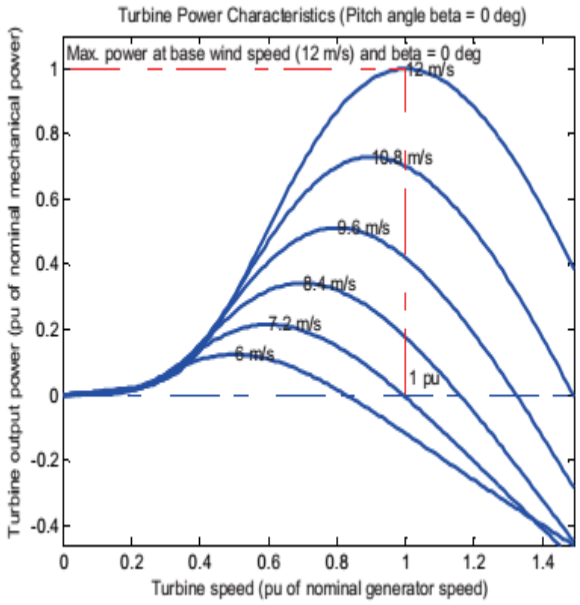

Fig.4the mechanical power versus the turbine speed

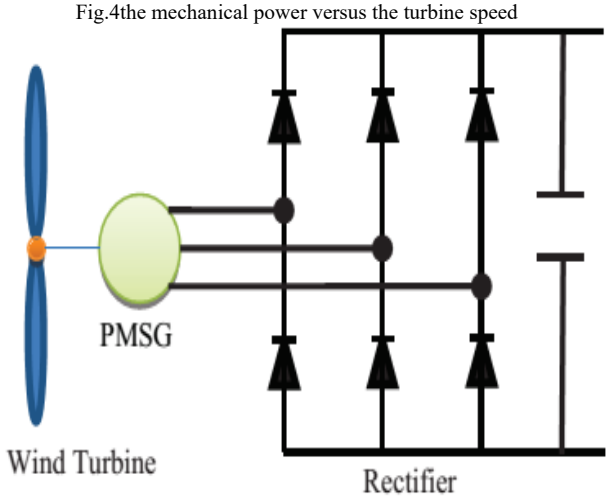

Fig.5 the wind turbine connected to a rectifier through PMSG

d) The Mathematical Model of the Parallel Inverters

The average model of the phase leg is derived based on the switching averaging. After transformation of the variables in the stationary coordinates Xabc into the rotating coordinatesXdqz, the average model can be simplified [15, 16 and 17] based on iz= iz1 = -iz$_2$≈ 0:

$$\frac{d}{dt}\begin{bmatrix}\tilde{i}_{d1}\\ \tilde{i}_{q1}\end{bmatrix}=\frac{1}{L_1}\begin{bmatrix}\tilde{d}_{d1}\\ \tilde{d}_{q1}\end{bmatrix}V_{dc1}-\frac{1}{L_1}\begin{bmatrix}\tilde{v}_d\\ \tilde{v}_q\end{bmatrix}-\begin{bmatrix}0 & -\omega\\ \omega & 0\end{bmatrix}\cdot\begin{bmatrix}\tilde{i}_{d1}\\ \tilde{i}_{q1}\end{bmatrix} \quad (15)$$

$$\frac{d}{dt}\begin{bmatrix}\tilde{i}_{d2}\\ \tilde{i}_{q2}\end{bmatrix}=\frac{1}{L_2}\begin{bmatrix}\tilde{d}_{d2}\\ \tilde{d}_{q2}\end{bmatrix}V_{dc2}-\frac{1}{L_2}\begin{bmatrix}\tilde{v}_d\\ \tilde{v}_q\end{bmatrix}-\begin{bmatrix}0 & -\omega\\ \omega & 0\end{bmatrix}\cdot\begin{bmatrix}\tilde{i}_{d2}\\ \tilde{i}_{q2}\end{bmatrix} \quad (16)$$

$$\frac{d}{dt}\begin{bmatrix}\tilde{v}_d\\ \tilde{v}_q\end{bmatrix}=\frac{1}{2C}\left(\begin{bmatrix}\tilde{i}_{d1}\\ \tilde{i}_{q1}\end{bmatrix}+\begin{bmatrix}\tilde{i}_{d2}\\ \tilde{i}_{q2}\end{bmatrix}\right)-\begin{bmatrix}\frac{1}{RC} & -\omega\\ \omega & \frac{1}{RC}\end{bmatrix}\cdot\begin{bmatrix}\tilde{v}_d\\ \tilde{v}_q\end{bmatrix} \quad (17)$$

Writing (15), (16) and (17) in general matrix form:

$$\dot{\tilde{\mathbf{x}}}=\mathbf{A}\tilde{\mathbf{x}}+\mathbf{B}\tilde{\mathbf{u}} \quad (18)$$

$$\tilde{\mathbf{y}}=\mathbf{C}\tilde{\mathbf{x}} \quad (19)$$

The state vector and the control vector are given as:

$$\tilde{\mathbf{x}}=[\tilde{v}_d \quad \tilde{v}_q \quad \tilde{i}_{d1} \quad \tilde{i}_{q1} \quad \tilde{i}_{d2} \quad \tilde{i}_{q2}]^T$$

$$\tilde{\mathbf{u}}=[\tilde{d}_{d1} \quad \tilde{d}_{q1} \quad \tilde{d}_{d2} \quad \tilde{d}_{q2}]^T$$

C = I, the matrices A, B can be obtained as:

$$\mathbf{A}=\begin{bmatrix}-1/RC & \omega & 1/(2C) & 0 & 1/(2C) & 0\\ -\omega & -1/RC & 0 & 1/(2C) & 0 & 1/(2C)\\ -1/L_1 & 0 & 0 & \omega & 0 & 0\\ 0 & -1/L_1 & -\omega & 0 & 0 & 0\\ -1/L_2 & 0 & 0 & 0 & 0 & \omega\\ 0 & -1/L_2 & 0 & 0 & -\omega & 0\end{bmatrix} \quad (20)$$

$$\mathbf{B}=\begin{bmatrix}0 & 0 & V_{dc1}/L_1 & 0 & 0 & 0\\ 0 & 0 & 0 & V_{dc1}/L_1 & 0 & 0\\ 0 & 0 & 0 & 0 & V_{dc1}/L_1 & 0\\ 0 & 0 & 0 & 0 & 0 & V_{dc1}/L_1\end{bmatrix}^T \quad (21)$$

III. THE DISTRIBUTED CONTROL

In the distributed control strategy the first and the second inverter have two control loops as shown in Figure.6. The inner control loops independently regulate the inverter output current in the rotating reference frame, id and iq. The outer loop works in the voltage control mode to produce the d-q axis current references for the inner loop by regulating the voltage at given reference value. In power control mode, the outer loop is used to regulate the active and the reactive power at given operating points and provide the current references, id-refandiq-ref, in the rotating reference frame for the inner

International Journal of Research
Available at https://edupediapublications.org/journals
e-ISSN: 2348-6848
p-ISSN: 2348-795X
Volume 04 Issue-17
December 2017

loop. The SVPWM is used to derive the six pulses where a PI controller scheme is used. The duty cycles signals are given as:

$$\tilde{d}_{d1}\cdot V_{dc1}=\left(K_{idp1}+K_{idi1}/s\right)\left(\tilde{i}_{d1-ref}-\tilde{i}_{d1}\right)-\omega L_1\tilde{i}_{q1}+\tilde{v}_d \quad (22)$$

$$\tilde{d}_{q1}\cdot V_{dc1}=\left(K_{iqp1}+K_{iqi1}/s\right)\left(\tilde{i}_{q1-ref}-\tilde{i}_{q1}\right)+\omega L_1\tilde{i}_{d1}+\tilde{v}_q \quad (23)$$

The voltage control loop regulates the voltage and generates the d-q axis current references for the current loop. Therefore the output of the outer voltage controller is the input of the inner control loop, a proportional-integral (PI) controller is also used in the current control loop. Then:

$$\tilde{i}_{d1-ref}=\left(K_{vdp}+K_{vdi}/s\right)\left(\tilde{v}_{d-ref}-\tilde{v}_d\right) \quad (24)$$

$$\tilde{i}_{q1-ref}=\left(K_{vqp}+K_{vqi}/s\right)\left(\tilde{v}_{q-ref}-\tilde{v}_q\right) \quad (25)$$

The second inverter operates in the power control mode, where the instantaneous values of the inverter output current components id-ref and iq-ref are used to control the output active and the reactive power respectively as shown in Figure 6. The duty-cycle signals for the second inverter are given as:

$$\tilde{d}_{d2}\cdot V_{dc2}=\left(K_{idp2}+K_{idi2}/s\right)\left(\tilde{i}_{d2-ref}-\tilde{i}_{d2}\right)-\omega L_2\tilde{i}_{q2}+\tilde{v}_d \quad (26)$$

$$\tilde{d}_{q2}\cdot V_{dc2}=\left(K_{iqp2}+K_{iqi2}/s\right)\left(\tilde{i}_{q2-ref}-\tilde{i}_{q2}\right)+\omega L_2\tilde{i}_{d2}+\tilde{v}_q \quad (27)$$

In the power control mode the active and the reactive power are controlled at given set points by the outer loops to produce the d-q axis current references for the inner loops ([16] and[17]). The active and the reactive power are given as:

$$P=(3/2)\left(V_d i_{d2}+V_d i_{q2}\right) \quad (28)$$

$$Q=(3/2)\left(V_q i_{d2}-V_d i_{q2}\right) \quad (29)$$

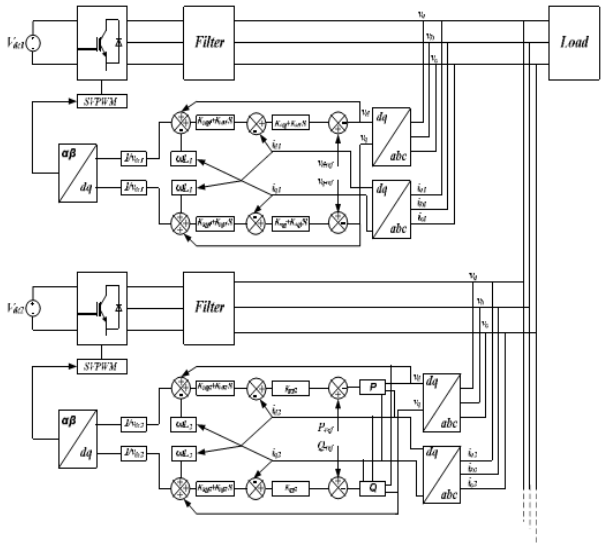

Fig.6. Closed-loop control of two Parallel Inverters

The outputs of these outer controllers are the inputs of the inner control loops. A proportional controller is used, and then we have:

$$\tilde{i}_{d2-ref}=K_{Pp2}\left(P_{ref}-P_2\right) \quad (30)$$

$$\tilde{i}_{q2-ref}=K_{Qp2}\left(Q_{ref}-Q_2\right) \quad (31)$$

In order to write the closed loop equation in matrix form, new control variables are introduced into (3.22)-(3.27). Then the new duty cycle signals can be expressed as:

$$\tilde{d}_{d1}=(1/V_{dc1})[\left(1-K_{idp1}K_{vdp}\right)\tilde{v}_d-K_{idp1}\tilde{i}_{d1}-\omega L_1\tilde{i}_{q1}+K_{idp1}K_{vdi}\tilde{\Phi}_{d1}+K_{idi1}\tilde{\gamma}_{d1}+K_{idp1}K_{vdp}\tilde{v}_{d-ref}] \quad (32)$$

$$\tilde{d}_{q1}=(1/V_{dc1})[\left(1-K_{iqp1}K_{vqp}\right)\tilde{v}_q-K_{iqp1}\tilde{i}_{q1}+\omega L_1\tilde{i}_{d1}+K_{iqp1}K_{vqi}\tilde{\Phi}_{q1}+K_{iqi1}\tilde{\gamma}_{q1}+K_{iqp1}K_{vqp}\tilde{v}_{q-ref}] \quad (33)$$

$$\tilde{d}_{d2}=(1/V_{dc1})[\left(1-1.5K_{idp2}K_{pp2}\tilde{i}_{d2}\right)\tilde{v}_d-1.5K_{idp2}K_{pp2}\tilde{i}_{q2}\tilde{v}_q-\left(1.5K_{idp2}K_{pp2}\tilde{v}_d+K_{idp2}\right)\tilde{i}_{d2}-\left(1.5K_{idp2}K_{pp2}\tilde{v}_q+\omega L_2\right)\tilde{i}_{q2}+K_{idi2}\tilde{\gamma}_{d2}+K_{idp2}K_{pp2}\tilde{P}_{ref}] \quad (34)$$

$$\tilde{d}_{q2}=(1/V_{dc2})[\left(1-1.5K_{iqp2}K_{Qp2}\tilde{i}_{d2}\right)\tilde{v}_q+1.5K_{iqp2}K_{Qp2}\tilde{i}_{q2}\tilde{v}_d+\left(1.5K_{iqp2}K_{Qp2}\tilde{v}_d-K_{iqp2}\right)\tilde{i}_{q2}-\left(1.5K_{iqp2}K_{Qp2}\tilde{v}_q-\omega L_2\right)\tilde{i}_{d2}+K_{iqi2}\tilde{\gamma}_{q2}+K_{iqp2}K_{Qp2}\tilde{\Phi}_{ref}] \quad (35)$$

The control output can be expressed as:

International Journal of Research
Available at https://edupediapublications.org/journals
e-ISSN: 2348-6848
p-ISSN: 2348-795X
Volume 04 Issue-17
December 2017

$$\tilde{\mathbf{u}} = \mathbf{H} \cdot \tilde{\mathbf{z}} + \mathbf{J}(\tilde{v}_d \tilde{v}_q \tilde{P} \tilde{Q})_{ref} \quad (36)$$

Where;

$$\tilde{\mathbf{z}} = [\tilde{v}_d \tilde{v}_q \tilde{i}_{d1} \tilde{i}_{q1} \tilde{i}_{d2} \tilde{i}_{q2} \tilde{\Phi}_{d1} \tilde{\Phi}_{q1} \tilde{\gamma}_{d1} \tilde{\gamma}_{q1} \tilde{\gamma}_{d2} \tilde{\gamma}_{q2}]^T$$

Substituting the control laws in the state equation and writing the equations in s-domain:

$$\mathbf{z}(s)/\mathbf{R}(s) = (s\mathbf{I} - \mathbf{A}_1 - \mathbf{B}_1\mathbf{H})^{-1} \cdot \mathbf{B}_2 \quad (37)$$

Where: A1 and B1 are the state and the input matrices of the closed loop system.

$$\mathbf{R}(s) = [(\tilde{v}_d \tilde{v}_q \tilde{P} \tilde{Q}_{ref})](s)$$

IV. DIODE-CLAMPED MULTILEVEL NVERTER

An m-level diode-clamped multilevel inverter typically consists of m – 1 capacitors on the dc bus and produces m levels of the phase voltage [4]. A three-phase five-level structure of a DCMLI is shown in Fig.7. Each of the three phases of the inverter shares a common dc bus, which has been subdivided by four capacitors into five levels. The voltage across each capacitor is Vdc, and the voltage stress across each switching device is limited to Vdc through the clamping diodes. Table II lists the output voltage levels possible for one phase of the inverter with the negative dc rail voltage V0 as a reference. State condition 1 means the switch is on, and 0 means the switch is off. Each phase has five complementary switch pairs such that turning on one of the switches of the pair requires that the other complementary switch be turned off. The complementary switch pairs for phase leg andare (Sa1, Sa'1), (Sa2, Sa'2), (Sa3, Sa'3), and (Sa4, Sa'4).

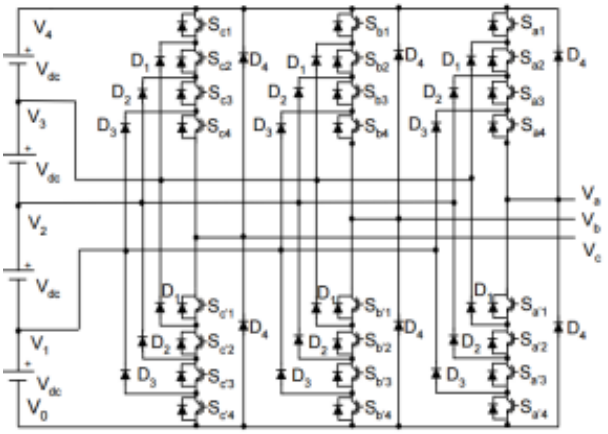

Fig.7.Athree-phase five-level diode-clamped multilevel inverter schematic

The following are the some advantages and disadvantages of the DCMLI:

Advantages:

- As the number of levels increases the harmoniccontent of the output waveform decreases the filter size.
- Lower switching losses due to the devices being switched at the fundamental frequency without increasing the harmonic content in the output.
- Reactive power flow can be controlled, as this doesnot cause unbalance in the capacitor voltages.
- Fast dynamic response.
- Back to back operation is possible.

Disadvantages:

- High number of clamping diodes is required as thenumber of levels increase.
- Active power transfer causes unbalance in the DC buscapacitors; this complicates the control of the system.

V. MATLAB/SIMULINK RESULTS

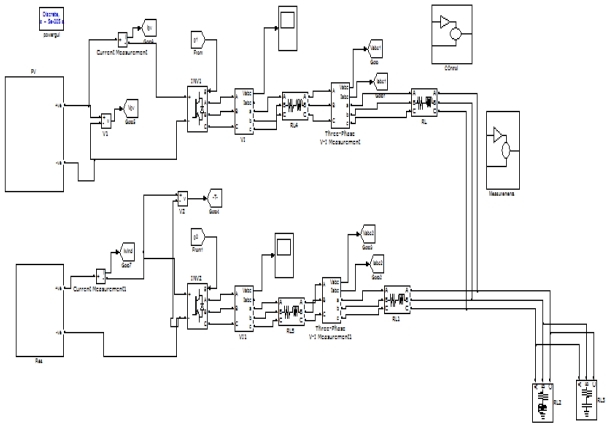

Fig.8 MATLAB/SIMULINK circuit for the PV/Wind MG

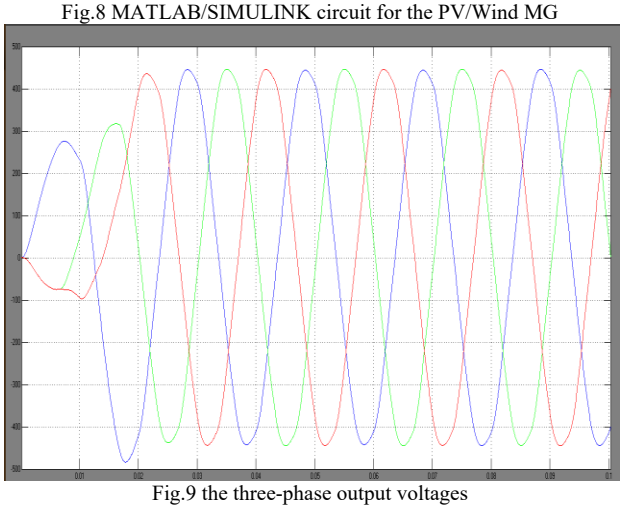

Fig.9 the three-phase output voltages

International Journal of Research
Available at https://edupediapublications.org/journals
e-ISSN: 2348-6848
p-ISSN: 2348-795X
Volume 04 Issue-17
December 2017

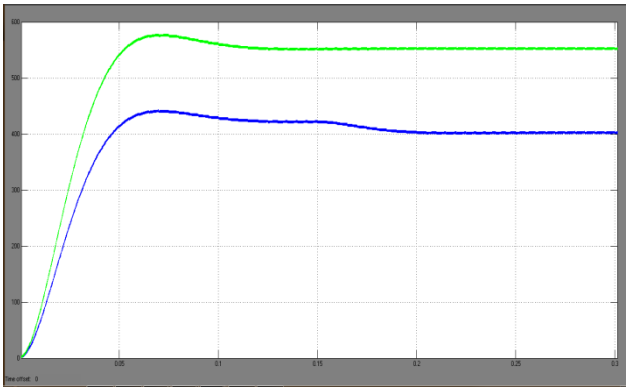

Fig.10 the DC input voltage of the inverters

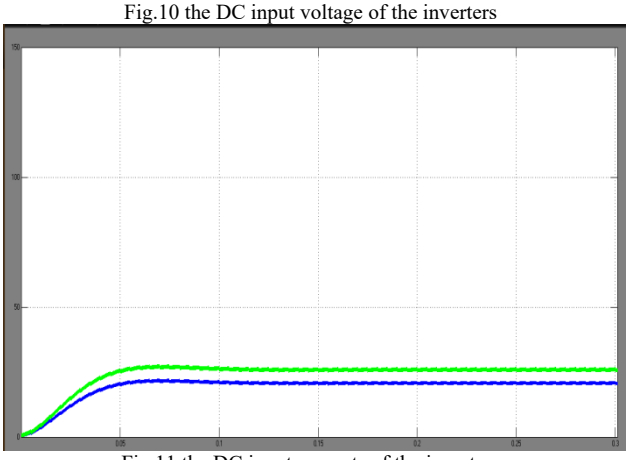

Fig.11 the DC input currents of the inverters

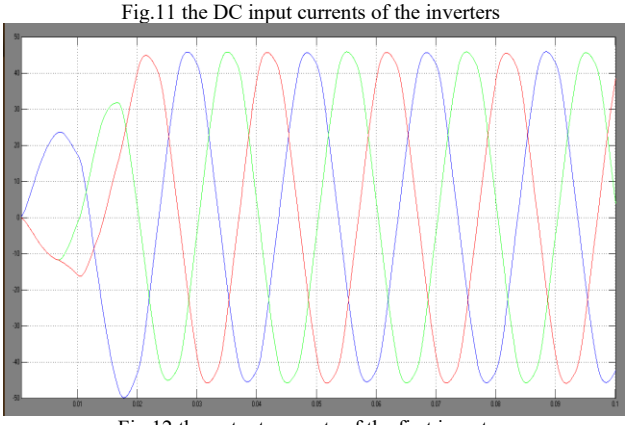

Fig.12 the output currents of the first inverter

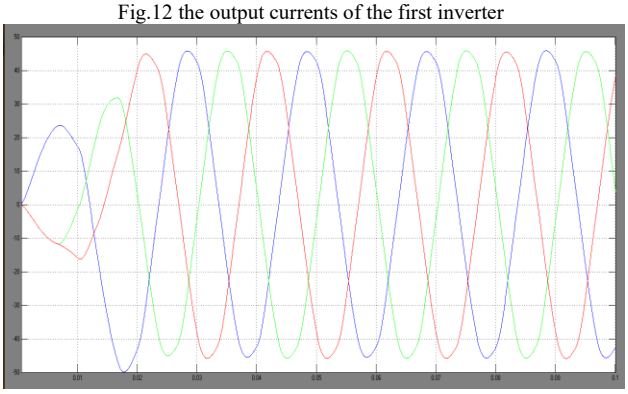

Fig.13 the output currents of the second inverter

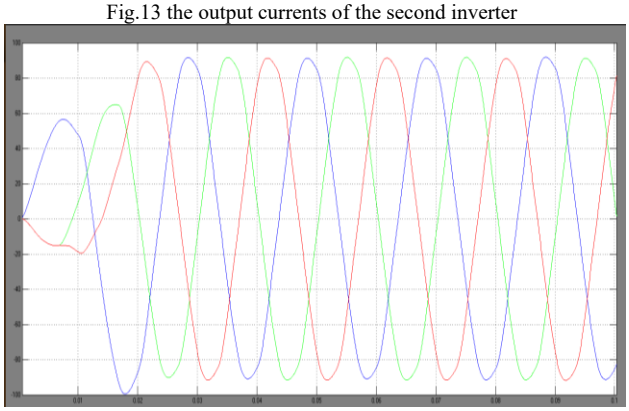

Fig.14 the output currents of the load

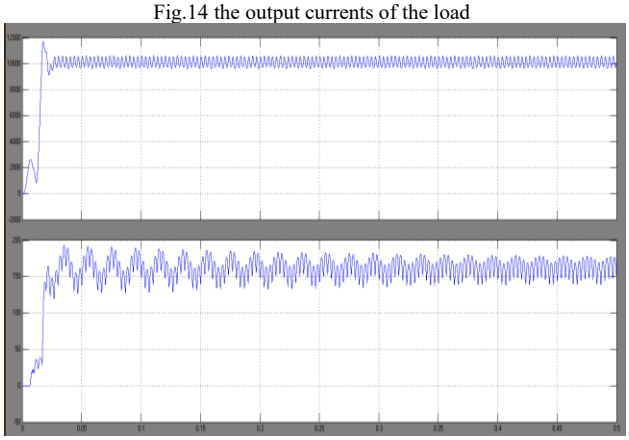

Fig.15 the active and the reactive power of first inverter

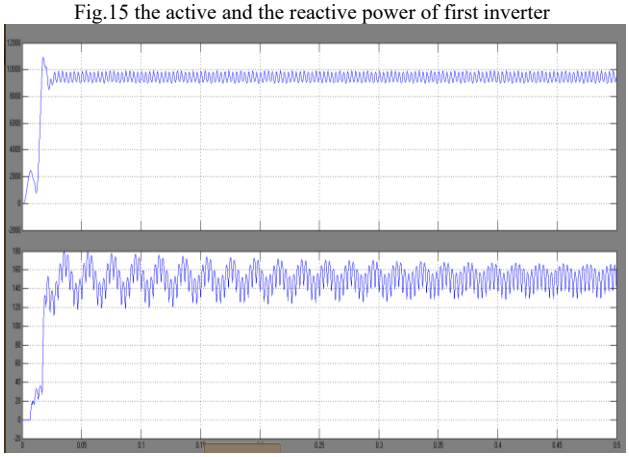

Fig.16 the active and the reactive power of second inverter

International Journal of Research
Available at https://edupediapublications.org/journals
e-ISSN: 2348-6848
p-ISSN: 2348-795X
Volume 04 Issue-17
December 2017

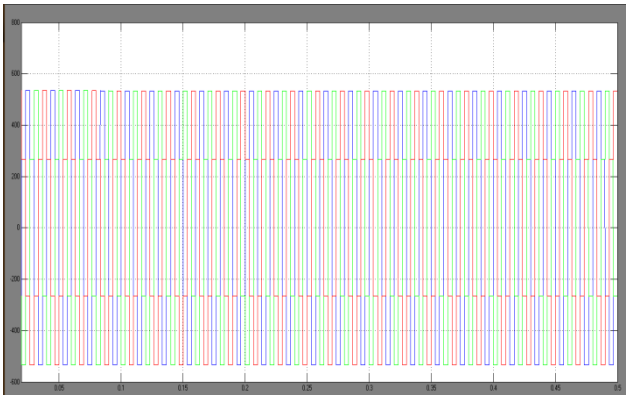

Fig.17 three phase inverter output voltage

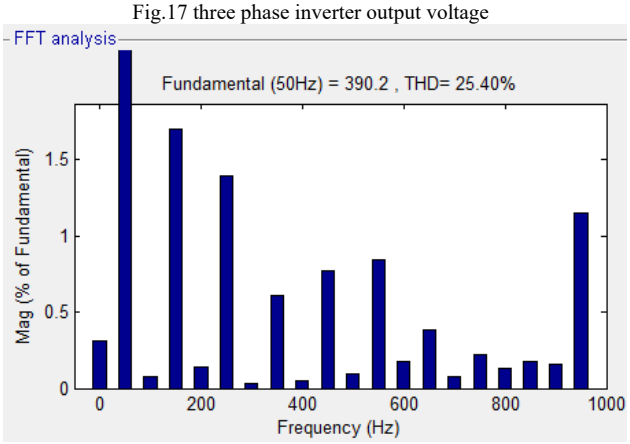

Fig.18 THD plot of three level inverter

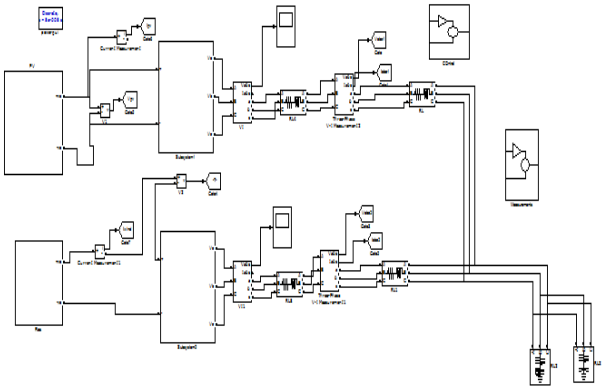

Fig.19 MATLAB/SIMULINK circuit for the PV/Wind MG with 5-level diode clamped multilevel inverter

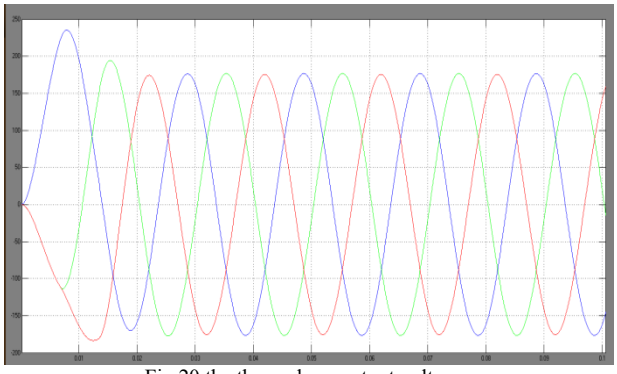

Fig.20 the three-phase output voltages

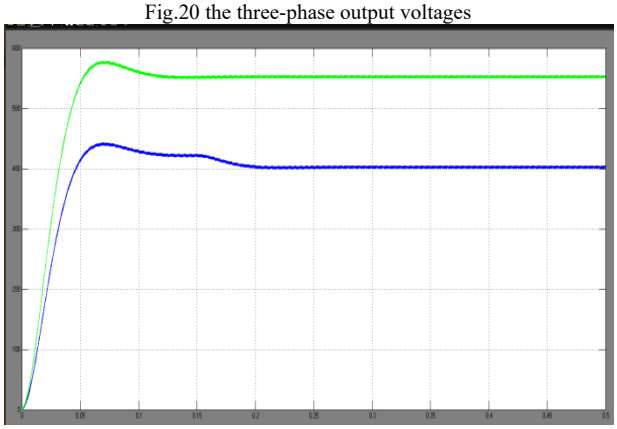

Fig.21 the DC input voltage of the inverters

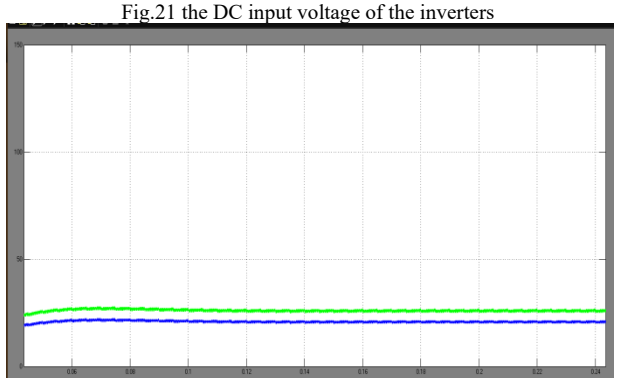

Fig.22the DC input currents of the inverters

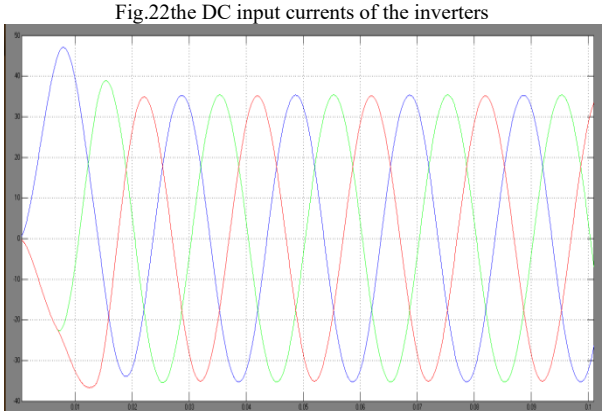

International Journal of Research
Available at https://edupediapublications.org/journals
e-ISSN: 2348-6848
p-ISSN: 2348-795X
Volume 04 Issue-17
December 2017

Fig.23 the output currents of the first inverter

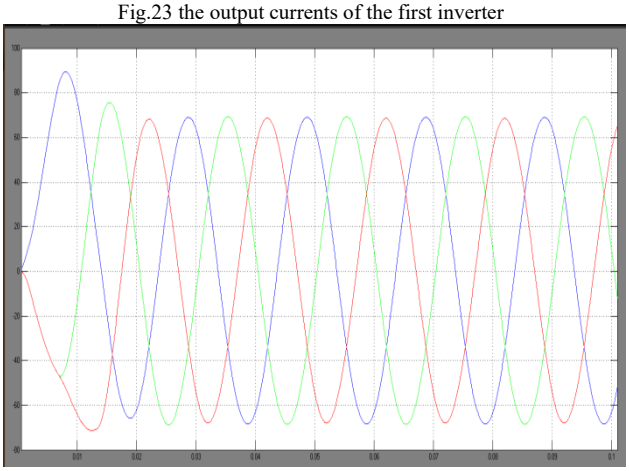

Fig.24 the output currents of the second inverter

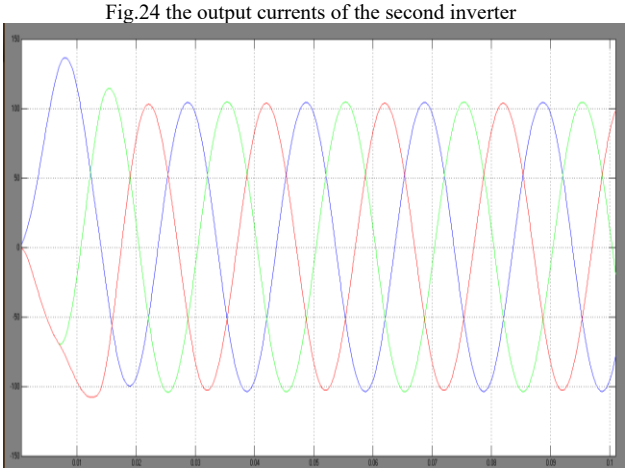

Fig.25 the output currents of the load

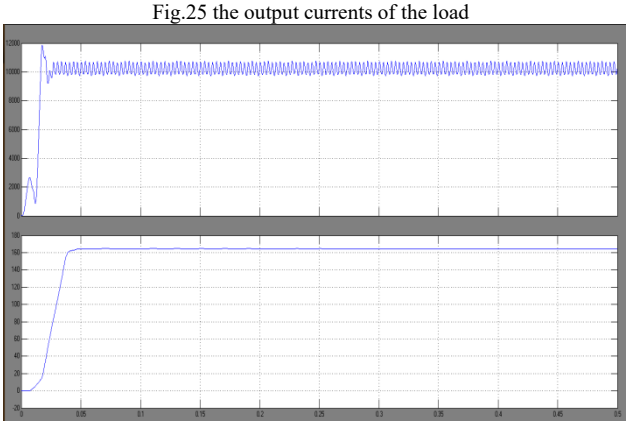

Fig.26 the active and the reactive power of first inverter

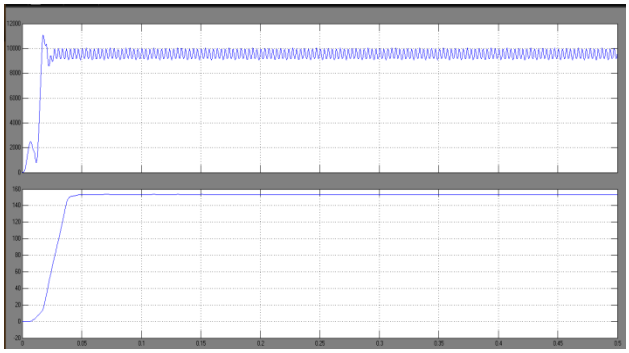

Fig.27 the active and the reactive power of second inverter

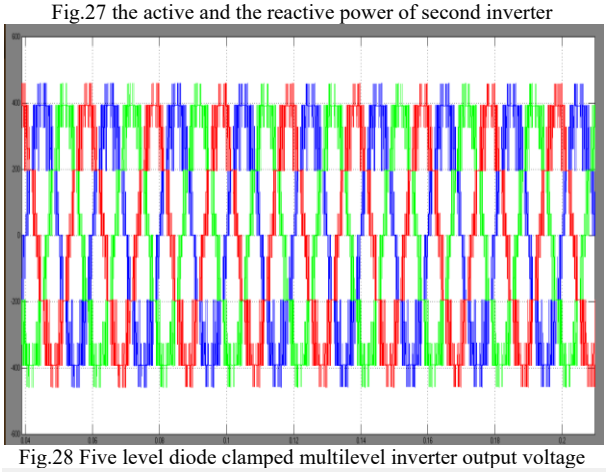

Fig.28 Five level diode clamped multilevel inverter output voltage

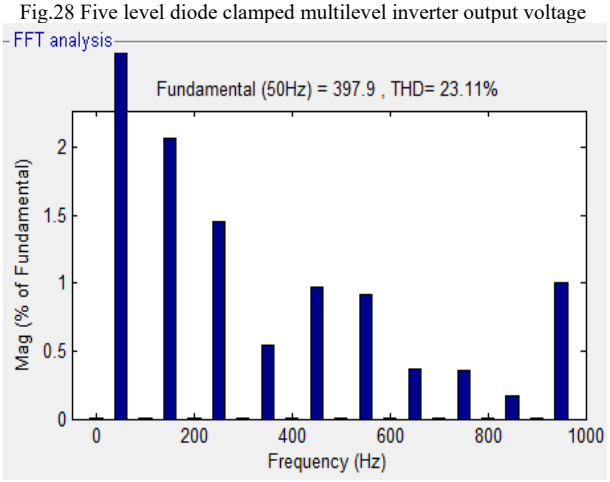

Fig.29 THD plot of five level inverter

VI. CONCLUSION

In this paper many topologies and control techniques have been reviewed, which helps the researchers to use proper techniques to control multilevel converters for grid integration.For ideal inverter connected voltage sources droop control can help in sharing real and reactive power.It is necessary to meet the energy need by utilizing the renewable energy resources like wind, biomass, hydro, co-generation, etc. In sustainable energy system, energy conservation and the use of renewable source are the key paradigm. With the increase in load demand, the

Renewable Energy Sources (RES) are increasingly connected in the distribution systems which utilizes power electronic Converters/Inverters. This paper has presented an overview of PV/wind. The model development of PV/wind module and arrays, power conditioning DC converter and the inverter set up. These designs are then integrated with an inverter controller that controls the voltage at a power system bus. The complete system is used as a micro-grid set up connected to a power grid. Modeling and evaluations of this model is conducted using 2, 3-levl and 5-level inverter modules. 5-level inverter topologies are tested using the Simulink. The results of these three inverter topologies are compared with 2, 3-level inverter with 5 –level and show that Percentage of THD in 5-level inverter is less.

REFERENCES

[1] Li.W., Ruan, X. Bao, C.Pan, D.Wang, X. Grid Synchronization Systems of Three-Phase Grid-Connected Power Converters: A Complex Vector-Filter Perspective. IEEE Transactions on Industrial Electronics, Volume 61, Issue: 4, IEEE Industrial Electronics Society, 2014, p.1855 - 1870.

[2] Yang, Y. Liu, G. Liu, H. Wang, W.Design and Simulation of three phase Inverter for grid connected Photovoltaic systems. IEEE, 11th World Congress on Intelligent Control and Automation (WCICA), 2014. June 29-July 4 2014, p.5453 – 5456.

[3] Zhilei Yao and Lan Xiao, Two-Switch Dual-Buck Grid-Connected Inverter With Hysteresis Current Control, IEEE Transactions on Power Electronics,vol 27, NO. 7, July 2012.

[4] E. Koutroulis, K. Kalaitzakis, N. C. Voulgaris, “Development of a microcontroller-based, photovoltaic maximum power point tracking control system”. IEEE Transactions Power Electronics, vol. 16, No 1, pp. 46-54, 2001.

[5] I. Houssamo, F. Locment, M. Sechilariu, “Maximum power tracking for photovoltaic power system: Developmentand experimental comparison of two algorithms”. Renewable Energy, vol. 35, No 10, pp. 2381-2387, 2010.

[6] T. A. Meynard, H. Foch, “Multi-level choppers for high voltage applications,” European Power Electronics Journal, vol. 2, no. 1, pp. 45-50, March 1992.

[7].J. M. Guerrero, M. Chandorkar, T-L. Lee, and P. C. Loh, "Advanced control architectures for intelligent micro grids-Part II: Power Quality, Energy Storage and AC/DC Micro grids," IEEE Trans. Ind. Electron., vol. 60, no. 4, pp. 1263-1270, Apr. 2013.

[8].M. Popov, H. Karimi, H. Nikkhajoei and V. Terzija, "Dynamic Model and Control of a Micro grid with Passive Loads", IPST Conference Proceedings, 2009.

[9].R. S. Alabri and E. F. El-Saadany, "Interfacing Control of Inverter-based DG Units", ICCCP-2009.

[10].J. M. Guerrero, M. Chandorkar, T-L. Lee and P. C. Loh, "Advanced control architectures for intelligent micro grids-Pqrt I: Decentralized and hierarchial control," IEEE Trans. Ind. Electron., vol. 60, no. 4, pp. 1254-1262,Apr. 2013.

[11].Xiongfei Wang, Josep M. Guerrero, Frede Blaabjerg, and Zhe Chen, "A Review of Power Electronics Based Micro grids," Journal of Power Electronics, Vol. 12, No. 1,January 2012 [6] "Evaluation of the Local Controller Strategies", micro grids. eu/ micro2000/ delivarables/ Deliverable DB2. Pdf.

[12].Xiao Zhao-xia, Fang Hong-wei, "Impacts of P-f & Q-V Droop Control on Micro Grids Transient Stability," Physics Procedia, vol. 24, pp. 276-282, 2012.

[13].Jose Mitas, Miguel Castilla, Luis Garcia de Vicuna, Jaume Miret, "Virtual Impedance Loop for Droop Controlled Single-Phase Parallel Inverters Using a Second Order General-Integrator Scheme," IEEE Transactions on Power Electronics, vol. 25, NO. 12, December 2010.